Adaptive Grid and Iterative Techniques for Submicron Device Simulation

Anand L. Pardhanani & Graham F. Carey
CFD Laboratory, WRW 301
The University of Texas, Austin, Texas 78712

Abstract

Numerical solution schemes based on adaptive grid redistribution and iterative techniques are investigated for submicron semiconductor devices. The grid adaptation strategy involves constructing a mathematical optimization problem to determine grid point locations. This is accomplished by defining an objective function which takes into account the numerical error and various geometric properties of the grid that affect accuracy. The iterative solution strategies considered here include multilevel nested iteration, and non-symmetric gradient-type iterative solvers for algebraic systems. Numerical tests are carried out using a non-parabolic hydrodynamic model for carrier transport.

Introduction

The use of adaptive gridding and iterative solution methods has proven very effective in many transport applications. Such techniques are particularly useful for problems involving multiple length scales or sharp solution gradients, which typically give rise to large algebraic systems. Semiconductor device applications are known to be grid-sensitive and they involve severe solution gradients, especially as device sizes shrink into the deep submicron regime. Thus, it is natural to consider iterative and adaptive grid approaches for device simulation.

Grid Adaptation

The present adaptive grid redistribution approach is developed using a discrete optimization model [2, 3]. This involves constructing a mathematical objective function that defines the desired grid properties, and then adjusting the grid to minimize this function. The optimization procedure is initiated by first computing an approximate solution using a simple initial grid, and then constructing an objective function based on a local feature or error indicator derived from this solution. The objective function takes into account properties of the numerical solution as well as geometric properties of the grid – for example, smoothness and orthogonality of grid lines – which may affect accuracy. The locations of the grid points constitute the unknowns in the objective function. For instance, a composite objective function which incorporates a measure of the solution error E, grid smoothness S and orthogonality O would be of the form

$$F(\boldsymbol{v}) = F(E(\boldsymbol{v}), S(\boldsymbol{v}), O(\boldsymbol{v})) \tag{1}$$

where $\boldsymbol{v}$ is a vector representing the grid point coordinates. Then the optimization problem can be stated as

$$\begin{aligned} &\text{minimize} \quad && F(\boldsymbol{v}) \\ &\boldsymbol{v} \in C \end{aligned} \tag{2}$$

Here C is the constraint set, which represents the space of all feasible grids with a given surface and boundary configuration. This constraint is needed to ensure, for example, that the redistributed nodes remain within the device domain, and to preserve the boundary or interface geometry.

The objective function may be generalized to include additional properties, and there are a variety of approaches for constructing its individual components. For example, $S(\boldsymbol{v})$ and $O(\boldsymbol{v})$ in (1) may be defined using a geometric approach, which can be illustrated in 2D with the help of Figure 1. The figure shows a representative patch of four cells surrounding any interior grid point (i,j). Local functions for the smoothness and orthogonality may be defined as:

$$\begin{aligned} S_{ij} &= r_1 \cdot r_1 + r_2 \cdot r_2 + r_3 \cdot r_3 + r_4 \cdot r_4 \\ O_{ij} &= (r_1 \cdot r_2)^2 + (r_2 \cdot r_3)^2 + (r_3 \cdot r_4)^2 + (r_4 \cdot r_1)^2 \end{aligned} \tag{3}$$

where r_i are the vectors shown in Figure 1. Similarly, a local feature/error adaptivity indicator w_{ij} can be defined at (i,j) and scaled by the local Jacobian (which is related to the patch area) to construct the adaptivity measure

$$E_{ij} = w_{ij} J_{ij}^2 \tag{4}$$

The functions in (3) and (4) can be accumulated over the entire grid to obtain global measures, and the objective function may be defined as a linear combination:

$$F(\boldsymbol{v}) = \alpha E(\boldsymbol{v}) + \beta S(\boldsymbol{v}) + \gamma O(\boldsymbol{v}) \tag{5}$$

with α, β and γ being positive constants that may be chosen to enforce adaptivity, smoothness and orthogonality to varying degrees.

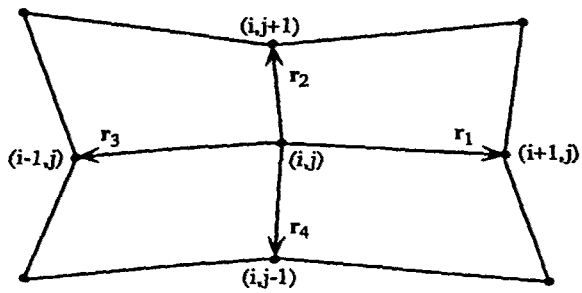

Figure 1: Representative interior patch of 4 cells around grid-point (i,j).

This formulation permits adapting the grid to the error or any desired feature of the problem. For example, in the semiconductor device problem a natural choice is to use the doping profile to adapt the initial grid as indicated in Figure 2.

Hydrodynamic Model and Discretization

The semiconductor device model used in our numerical experiments consists of the non-parabolic hydrodynamic transport system developed by Bordelon et al. [1]. The resulting coupled Poisson and transport equations that relate the electrostatic potential (ϕ), carrier density (n), velocity $(\boldsymbol{v})$ and energy (w) have the following form:

$$\begin{aligned} \nabla \cdot (\epsilon \nabla \phi) &= q(n - N_D) \\ \frac{\partial n}{\partial t} + \nabla \cdot (n\boldsymbol{v}) &= 0 \\ \frac{\partial (A(w) n \boldsymbol{v})}{\partial t} + \frac{2}{3m^*} \nabla (B(w) n w) - \frac{q}{m^*} n \nabla \phi &= -\frac{n\boldsymbol{v}}{\tau_p} \\ \frac{\partial (nw)}{\partial t} + \nabla \cdot (\Omega n w \boldsymbol{v} + \boldsymbol{Q}) - qn\boldsymbol{v} \cdot \nabla \phi &= -n \frac{(w - w_0)}{\tau_w} \end{aligned} \tag{6}$$

with $A(w) = 1 + 2\Omega\alpha w$, $B(w) = (1 + \alpha w)/(1 + 2\alpha w)$, $\boldsymbol{Q}$ = "heat flux" $= -nD_w\nabla w$, and with empirical constants $\alpha = 0.5eV^{-1}$, $\Omega = 1.3$ and $D_w \sim 10$ cm^2/sec.

In the present work, the equation system is first analytically mapped to a reference domain to facilitate discretization on general non-uniform grids. The spatial derivatives and metrics in the transformed equations are then discretized using second-order finite-differencing. We use an extension of the Scharfetter-Gummel treatment for the current density and energy flux. For the hydrodynamic system (6), following the usual procedure, we assume locally constant current density and electric field, and linear variation in energy. This yields an approximation of the form

$$\begin{aligned} nv &= \left[\frac{n_{i+1}}{w_{i+1}}B(-\Delta_J) - \frac{n_i}{w_i}B(\Delta_J)\right]\frac{c_1\frac{dw}{d\xi}}{\ln(w_{i+1}/w_i)} \\ \Delta_J &= \left(2 + (c_2\frac{d\phi}{d\xi})/(c_1\frac{dw}{d\xi})\right)\ln(w_{i+1}/w_i) \end{aligned} \tag{7}$$

where subscripts i and $i+1$ denote nodal values in the reference coordinate direction ξ, c_1 and c_2 are coefficients in the scaled momentum equation, and $B(x) = x/(e^x - 1)$ denotes the Bernoulli function. Similarly, assuming locally constant energy flux (S) and exponential n one can derive the approximation

$$\begin{aligned} S &= [w_{i+1}B(-\Delta_S) - w_iB(\Delta_S)]\frac{d_2\nu}{\delta\xi} \\ \Delta_S &= (d_1\delta\xi)/(d_2\nu) \\ \nu &= \ln(n_{i+1}/n_i)\,[n_{i+1}\ n_i/\ (n_{i+1} - n_i)] \end{aligned} \tag{8}$$

where d_1 and d_2 are coefficients in the scaled energy equation. The resulting semi-discrete equation system is integrated to steady state in a fully-coupled form using backward Euler or semi-implicit Runge-Kutta schemes.

Iterative solution

Solution techniques of special interest in the present work include multigrid-type schemes as well as generalized gradient iterative solvers. Multigrid techniques are based on the use of a sequence of nested grids over the given domain, and solving the problem using a cyclic iterative process which exploits each grid's preferential convergence behavior [4]. The resulting algorithm is usually far more efficient than traditional single-grid iterative algorithms. In this work we focus on nested grid schemes, wherein the solution process begins most economically at the coarsest level and proceeds to finer levels using projection to generate good starting iterates. Figure 3 shows sample results obtained using a two-grid scheme to solve the non-parabolic hydrodynamic model for a 0.08 micron (channel-length) $n^+ - n - n^+$ diode structure. In this example we first computed a drift-diffusion solution on the coarse grid for use as initial approximation to the coarse grid hydrodynamic solution. This was interpolated to the fine grid using an approach consistent with the Scharfetter-Gummel assumptions.

Generalized gradient iterative methods such as bi-conjugate gradients (BCG) and conjugate gradient squared (CGS) are also under investigation. Implicit integration of the fully-coupled hydrodynamic system yields large block-structured algebraic systems at each integration step, which must be solved efficiently for enhancing the efficiency of the overall simulation process. For a simple MOSFET test case such as the one shown in Fig. 2, preliminary calculations have shown an order of magnitude improvement on a 129×33 non-uniform grid when a CGS scheme is used instead of a band solver.

Acknowledgements

This research is being supported by the Semiconductor Research Corporation and the Texas Advanced Technology Program.

References

[1] T. J. Bordelon, X.-L. Wang, C. M. Maziar and A. F. Tasch, "Accounting for bandstructure effects in the hydrodynamic model: a first-order approach for silicon device simulation," *Solid-State Electronics,* vol. 35, no. 2, pp. 131-139, 1992.

[2] A. Pardhanani and G. F. Carey, "Optimization of computational grids," *Numerical Methods for Partial Differential Equations,* vol. 4, no. 2, pp. 95-117, 1988.

[3] A. Pardhanani and G. F. Carey, "Adaptive redistribution and multilevel techniques for time-dependent and steady problems," in *Multigrid Methods: Special Topics and Applications II,* GMD-Studien Nr. 189, GMD, Sankt Augustin, 1991.

[4] P. Wesseling, *An Introduction to Multigrid Methods,* John Wiley, Chichester (England), 1992.

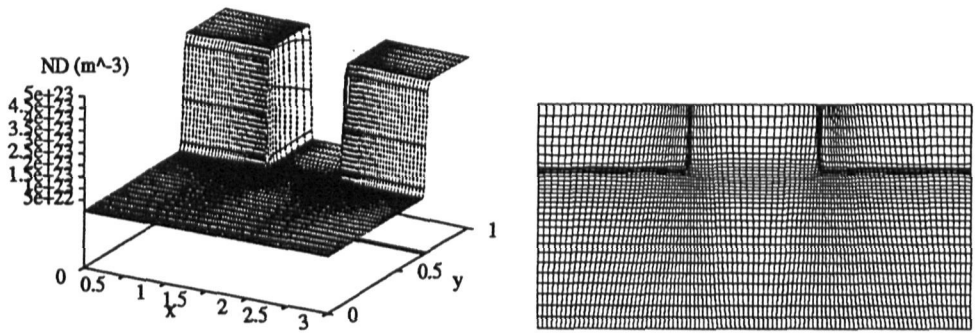

(a) (b)

Figure 2: (a) Representative MOSFET doping profile; and (b) grid adapted to doping.

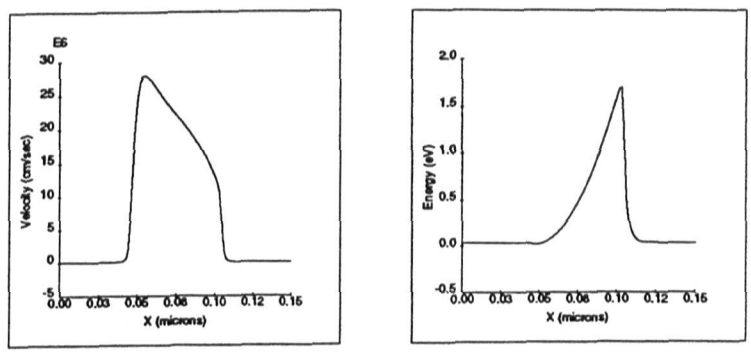

Figure 3: Hydrodynamic simulation of carrier velocity and energy at 3 volts bias for 0.08μm $n^+ - n - n^+$ diode with 129 grid points; doping concentration varies 5 orders of magnitude at junctions.